# Master Sintering Curve Concepts as Applied to the Sintering of Molybdenum

DEBORAH C. BLAINE, JOHN D. GUROSIK, SEONG JIN PARK, DONALD F. HEANEY, and RANDALL M. GERMAN

Sintering experiments with various molybdenum powders are rationalized using a master sintering curve concept that collapses density, grain size, or other parameters onto a single curve. In this case, the integral work of sintering is developed and customized for different green densities. Construction of the master sintering curve is described to show how the curve can be normalized with respect to green density effects. Various grades of molybdenum for metal injection molding and die compaction are included in the analysis, processed over a range of heating cycles. Die-compacted samples of varying green densities are used to illustrate the efficacy of the new, normalized master sintering curve concept. Sintering cycle optimization is one possible outcome from this analysis.

## I. INTRODUCTION

MATERIALS suited for high-temperature applications usually have high melting temperatures, making them difficult to manufacture by methods such as casting. Powder metallurgy techniques offer alternative processing routes that avoid melting, yet deliver net-shape products. A prime example of such a material is molybdenum.[1] Molybdenum has a melting temperature of 2622 °C, yet after consolidation, the powder can be sintered at temperatures near 2000 °C. Indeed, considerable sintering is evident at much lower temperatures. In materials that require such high sintering temperatures, it is attractive to design sintering cycles that minimize the energy consumption while attaining a target density. Also, minimizing the sintering time will reduce grain growth, giving better sintered strength and other properties.[2,3]

The master sintering curve is a model based on diffusion theories that links the work of sintering $\Theta$ to the relative density $\rho$ at any point in the sintering cycle.[4] The work of sintering needed to obtain a target density can be generated by various combinations of heating rate, hold time, and isothermal temperatures. Thus, once mapped for density *vs* the work of sintering, the master sintering curve enables process optimization.

Sintering behavior is typically influenced by parameters such as initial density $\rho_o$, particle size $D$, and grain size $G$. Variations between powder vendors and powder lots lead to noticeable changes in the sintering response. In this study, sintering of six different molybdenum powders from two different vendors is evaluated through master sintering curves constructed for each powder. Comparisons between these master sintering curves provide insight into the changes in sintering work due to changes in powders as well as green density and presintering treatments. We introduce a new method that normalizes the relative density data to eliminate green density effects on the master sintering curve. This provides a versatile tool for designing optimal sintering cycles.

DEBORAH C. BLAINE, Materials Research Engineer, formerly with the Center for Innovative Sintered Products, Pennsylvania State University, is with Bleistahl Productions GmbH & Co., Wetter D-58300, Germany. Contact e-mail: dcb193@psu.edu JOHN D. GUROSIK, Process Engineer, formerly with the Center for Innovative Sintered Products, Pennsylvania State University, is with GKN Sinter Metals, Emporium, PA 15857. SEONG JIN PARK, Research Professor, and RANDALL M. GERMAN, CAVS Professor and Director, formerly with the Center for Innovative Sintered Products, Pennsylvania State University, are with the Center for Advanced Vehicular Systems, Mississippi State University, Mississippi State, MS 39762-5405. DONALD F. HEANEY, Director Process Development, is with the Center for Innovative Sintered Products, Pennsylvania State University, University Park, PA 16802-6809.

Manuscript submitted July 15, 2004.

## II. MASTER SINTERING CURVE THEORY

Early research identified that diffusion plays the primary role in densification of a powder during sintering.[6] For the large majority of materials, either grain boundary or volume diffusion is the dominant densification mechanism. Surface diffusion is active with small powders, but it does not contribute to densification. The following multiple mechanism model provides a means to predict densification behavior:[4]

$$\frac{d\rho}{3\rho dt} = \frac{\gamma\Omega}{\mathrm{k}T}\left[\frac{\Gamma D_0}{(G)^n}\right]\exp\left(-\frac{Q}{\mathrm{k}T}\right) \qquad [1]$$

with $n = 3$ for volume diffusion, and $n = 4$ for grain boundary diffusion. In Eq. [1], $\gamma$ = surface energy, $\Omega$ = atomic volume, k = Botlzmann's constant, $\Gamma$ = material properties, $D_0$ = diffusivity pre-exponent, $G$ = grain size, $Q$ = apparent activation energy for diffusion, $t$ = time, and $T$ = absolute temperature. This model assumes grain growth can be described as a function of density only.[4] This assumption has received criticism because frequently grain growth is independent of densification, but during constant heating rate experiments below full density, this condition is applicable.[5] The master sintering curve is derived from this model as follows: Eq. [1] is rearranged to gather all the constants and material-dependent parameters, except for the apparent activation energy, into a single density-dependent parameter $\Phi$:

$$\Phi(\rho) \equiv \frac{\mathrm{k}}{\gamma\,\Omega\,D_o}\int_{\rho_o}^{\rho}\frac{(G)^n}{3\rho\Gamma}\,d\rho \qquad [2]$$

Integration is performed over the sintering range, from the initial or green density to the sintered density. The remaining terms are collected into a parameter that is equivalent to

the thermal work performed in reaching the sintered density. This parameter $\Theta$ is termed the work of sintering:

$$\Theta(t,T) \equiv \int_{t_0}^{t} \frac{1}{T} \exp\left(-\frac{Q}{kT}\right) dt \qquad [3]$$

Note that the work of sintering depends on the time-temperature pathway and contains a unique apparent activation energy. While the dominant sintering densification mechanism is volume or grain boundary diffusion, most materials densify through a mixture of densification mechanisms, each with changing roles during heating and as the microstructure changes. For example, grain boundary diffusion is sensitive to the grain size, so grain growth changes its contribution as the grain boundary area declines. Because of these mixed events and their complex dependence on temperature, grain size, surface area, and curvature, the apparent activation energy used in Eq. [3] often does not match a handbook diffusional parameter. Instead, the apparent activation energy is found through iteration. The apparent activation energy that yields the maximum coefficient of determination through regression analysis of experimental data to a sigmoid curve is selected for the master sintering curve.

## III. EXPERIMENTS

The sintering experiments examined four different grades of molybdenum powder from two different vendors.[1] Table I identifies the powders and gives the pycnometer density and median particle size. The metal injection molding (MIM) powders were milled to remove agglomerates before particle size measurement was conducted. Before milling, the mean particle size was similar for both the O-1 and H-1 powders; however, after milling, the difference in mean particle size was more distinct.[1] The ready-to-press (RTP) powders were supplied with the compaction lubricant already added, which causes the powder to be agglomerated in the as-received state. In the case of the H-2 powder, the powder was spray dried with a water soluble binder. The O-2 powder was prewaxed using a binder that is insoluble in water. The particle size measurements were performed using powders dispersed in water; thus, the O-2 powder agglomerates persisted while the H-2 powder agglomerates were partially dispersed. This explains the large difference in mean particle size measured for these two powders.

Both die compaction and injection molding were used to form samples. The powder injection molding feedstock was formulated using the milled H-1 and O-1 powders with a standard wax-polymer binder at a 52 vol pct solids loading. Tensile bars with a cross section of 6.5 by 3.2 mm and gage length 25.4 mm were injection molded from the feedstocks. After molding, the PIM samples were solvent debound in heptane at 60 °C for a minimum of 4 hours prior to further processing.

Other tensile bars were fabricated from the H-2 and O-2 powders using die compaction. The agglomerated powders were passed through a 100 mesh sieve. Tensile bars with 645 $mm^2$ projected area and 6.35-mm thickness were pressed at different pressures to obtain the desired range of green densities. Samples were pressed to relative green densities of 0.55, 0.60, 0.65, 0.70, and 0.75.

All samples were subjected to a combined polymer burnout and presintering cycle. This was under flowing hydrogen with a cycle consisting of the following: heat 5 °C/min to 250 °C, hold 1 hour, heat 3 °C/min to 450 °C, hold 2 hours, heat 10 °C/min to 1000 °C, hold 30 minutes. Subsequent separate heating in hydrogen was used to remove any oxygen or carbon contamination from the polymer burnout cycle, using a cycle of 10 °C/min to 1000 °C, hold 20 minutes, heat 3 °C/min to 1400 °C, hold 2 hours. Cooling was at 10 °C/min to room temperature.

Final sintering densification was in a graphite element vacuum furnace operating at 0.13 Pa pressure. The samples were enclosed in a molybdenum box to minimize impurity pickup. For construction of the master sintering curve, several experimental points were captured during sintering densification. The baseline sinter cycle was 10 °C/min to 1400 °C with a final hold of 20 minutes. Sintering above 1400 °C followed directly on from the baseline sinter cycle, ramping at varying rates to varying peak temperatures. These cycles are tabulated in Table II, and were determined by a design of experiments matrix using three ramp rates: 1 °C/min, 2 °C/min, and 5 °C/min; three peak sintering temperatures: 1600 °C, 1700 °C, and 1800 °C; and three peak hold times: 1, 2, and 10 hours.[1]

**Table II. Master Sintering Curve Sintering Cycles**

| Peak Temperature (°C) | Ramp Rate from 1400 °C (°C/min) | Hold Time at Peak Temperature (h) |
|---|---|---|
| 1600 | 1 | 1 |
| 1600 | 2 | 10 |
| 1600 | 5 | 2 |
| 1700 | 1 | 10 |
| 1700 | 2 | 2 |
| 1700 | 5 | 1 |
| 1800 | 1 | 2 |
| 1800 | 2 | 1 |
| 1800 | 5 | 10 |

**Table I. Manufacturer, Designation, Density, and Symbol for Molybdenum**

| Powder | Manufacturer | Designation | Pycnometer Density ($g/cm^3$) | Median Particle Size ($\mu m$) |
|---|---|---|---|---|
| H-1 | HC Starck | MIM (milled) | 10.26 | 3.4 |
| H-2 | | RTP | 10.20 | 14 |
| O-1 | Osram Sylvania | 490/100 MIM (milled) | 10.22 | 2.8 |
| O-2 | | 490/100 RTP | 10.20 | 23 |

RTP: ready to press powder with preaddition of lubricant.
MIM: metal injection molding grade powder.

Additional vacuum sintering cycles were run to 1100 °C, 1200 °C, or 1300 °C with a 2-hour hold at temperature to create some intermediate data points. Those lower temperature samples did not undergo the oxygen and carbon removal treatments mentioned earlier.

Archimedes density measurements were used to determine the sintered density.

## IV. CONSTRUCTION OF THE MASTER SINTERING CURVE

Density data collected from sintering experiments are used to construct the master sintering curve. The pycnometer density was used for the theoretical density $\rho_{th}$ for each powder. The relative density $\rho$ is the ratio of the sintered density $\rho_s$ to the theoretical density,

$$\rho = \frac{\rho_s}{\rho_{th}} \qquad [4]$$

For any time-temperature pathway, it is possible to calculate the work of sintering $\Theta$ in Eq. [3] for any point where the density is measured. Thus, the work of sintering in Eq. [3] is calculated for each experimentally measured density point by knowing the time-temperature pathway. Using numerical integration and the trapezoidal rule, the work of sintering is approximated as

$$\Theta \equiv \sum_{i=0}^{i=n} \frac{I_i + I_{i+1}}{2} (t_{i+1} - t_i) \qquad [5]$$

where $I$ is the integrand of Eq. [3] and $n$ is the number of intervals the domain is divided into. The relative density, calculated by Eq. [4], is plotted against the natural logarithm of the work of sintering to form the master sintering curve. The apparent activation energy is determined and used to collapse all of the data onto a single curve, which is then fit with a sigmoid function to create a custom linkage between the sintering parameter such as density and the integral work of sintering.

A sigmoid curve has consistently demonstrated the best fit to density *vs* work of sintering integral. Thus, the relative density $\rho$ is fitted to the sigmoid form as follows:

$$\rho = a + \frac{1 - a}{1 + \exp\left(-\frac{(\ln \Theta - b)}{c}\right)} \qquad [6]$$

The constants *a, b*, and *c* define the master sintering curve for the system. Constant *a* is the initial relative density. Constants *b* and *c* are determined using the generalized Newton–Rhapson method by minimizing the norm,

$$\text{Err} = \left( \sum_{i=1}^{N} (\rho_i/\rho - 1)^2/N \right)^{1/2} \qquad [7]$$

where $\rho_i$ refers to the experimentally measured relative density, and $\rho$ refers to the predicted value using Eq. [6].

While it was initially thought that volume diffusion was the dominant sintering mechanism in the densification of pure molybdenum, studies on activated sintering showed that grain boundary mobility retarded densification, thus causing the apparent activation energy to be driven up to values that seemed more in line with volume diffusion.[2,3,7–10] The current consensus is that grain boundary diffusion is considered to be the dominant densification mechanism for most materials.[6] Constant heating rate experiments used to measure activation energies can be misleading because grain growth influences are not incorporated in these measurements. Sintering of pure molybdenum occurs dominantly by grain boundary diffusion (activation energy of 263 kJ/mol) and surface diffusion (activation energy of 241 kJ/mol).[6] Because surface diffusion consumes the sintering potential during the initial stages without contributing to densification, the apparent activation energy for densification is higher, as routinely observed in sintering.[9] Because of the surface diffusion impediment to densification, it is usually necessary to apply pressure *via* HIP (hot isostatic pressing) to achieve full density. For this study, the apparent activation energy used in Eq. [3] to calculate the work of sintering is 290 kJ/mol. Figure 1 shows the coefficient of determination for various apparent activation energies applied to the molybdenum experiments conducted. The 290 kJ/mol value gives the best regression analysis fit and lies somewhere between the grain boundary and volume diffusion activation energy values.

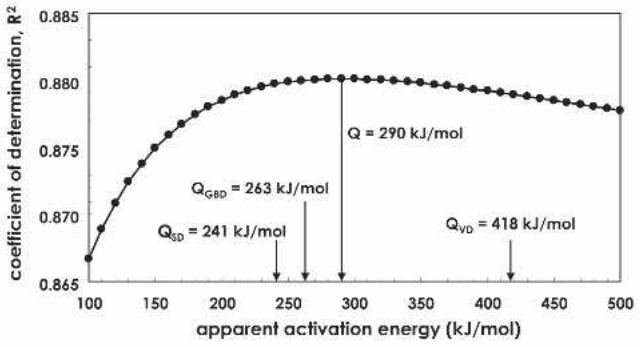


Fig. 1—Determination of apparent activation energy used in master sintering curve by using regression analysis.

## V. NORMALIZATION OF THE MASTER SINTERING CURVE

Normalization of the relative density reveals some predictive aspects that link differing starting conditions. This is done through the following normalizing equation:

$$\rho_n = \frac{\rho - 1}{(1 - \rho_0)} + 1 \qquad [8]$$

where $\rho_n$ is the normalized relative density, and $\rho_0$ is the initial relative density. From Eq. [8], it can be shown that normalization converts each data set to vary between an arbitrary value of 0 at the initial condition of $\rho = \rho_0$, and 1 at the upper limit, $\rho = 1$, where the relative density approaches the theoretical density of the material. In essence, the normalized relative density indicates the degree to which a compact approaches theoretical density relative to its initial state.

Because each powder has its own unique densification character, normalization of the master sintering curve data causes the individual master sintering curves to collapse into a single curve. Using the normalized master sintering curve, time-temperature-density maps are constructed independent

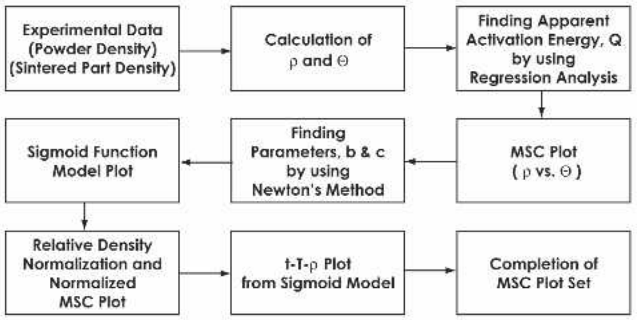


Fig. 2—Overall algorithm for molybdenum master sintering curve construction.

of initial density. Figure 2 is a flowchart showing the overall process for constructing the master sintering curve from the experimental data, normalizing the data, and constructing the time-temperature-density maps from the normalized master sintering curves.

## VI. RESULTS AND DISCUSSION

The experimental procedures create a large quantity of data. To identify specific influences, certain sets of data were isolated for direct comparison.

Figure 3 plots the relative density *vs* work of sintering for the MIM (metal injection molding) grade powders, H-1 and O-1. The master sintering curve is overlaid on these data. These results show that O-1 powder densifies at a faster rate and reaches a higher final density than the H-1 powder for the same sintering work Θ. The master sintering curves indicate any difference in sintered density is lost as full density is approached.

Figure 4 compares thermally debound and undebound die compacted samples fabricated from the H-2 powder. The undebound samples show a slightly retarded sintering response. The debound samples experienced enhanced sintering rates, but final density was similar at high values for the work of sintering. The enhanced sintering rates can be attributed to the absence of carbon in the debound samples as compared to the undebound samples. The final undebound samples showed the presence of carbides.

For these two initial analyses, the effect of initial density was removed by comparing samples with similar initial densities. The effect of varying initial density can be isolated by comparing the density data of samples die compacted using the H-2 powder at different green densities. Figure 5(a) plots the data to show that a lower green density leads to faster densification. However, independent of the initial density, the densification curves converge to the same value.

Normalization of the relative density data according to Eq. [8] gives a single curve, as shown in Figure 5(b). The success of this normalization procedure allows differences in green density to be handled with one master sintering curve. Each such curve is powder specific, but allows accurate prediction of the sintered density even for varying green densities. This trend is confirmed through similar analysis of the O-2 powder, as demonstrated in Figure 6. Thus, normalized master sintering curves have been identified that are not constrained to a constant green density.

Figure 7 plots the normalized curves for each powder included in this study. Comparison of the normalized

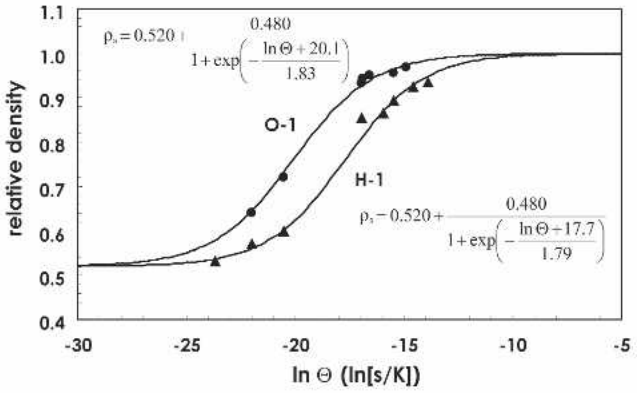


Fig. 3—Comparison in the sintering response between H-1 and O-1 PIM grade powders.

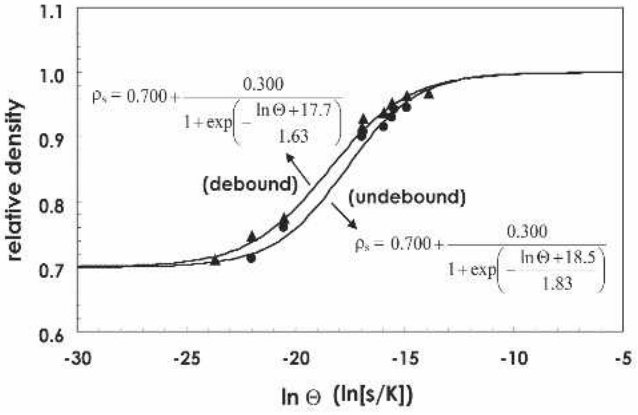


Fig. 4—Comparison of H-2 powder sintered with and without a polymer burnout cycle pretreatment—debound and undebound.

curves allows general comparison of the sintering capabilities of various powders. A difference in powder vendors is evident, which appears to trace to the particle size. Particle size significantly influences densification, with smaller particles inducing higher densification rates.[3] The particle size listed for the O-2 RTP powder in Table I is the agglomerated particle size. The MIM grade O-1 powder was used to form the O-2 RTP powder; however, the agglomeration that occurs after adding the compaction lubricant causes the difference in measured particle size seen in Table I. Milled particle sizes and scanning electron micrographs of the powders offer evidence in support of this observation.[1]

From Figure 7, it is also apparent that the MIM grade powders (H-1 and O-1) sinter faster than the agglomerated RTP powders (H-2 and O-2) for each vendor. The implementation of the normalized master sintering curves greatly simplifies comparison between these powders, facilitating choosing between powders and vendors, and ultimately choosing between different sintering cycles.

Finally, in Figure 8, an example of a time-temperature-density map for a specific powder system is shown. The MIM grade H-1 and O-1 powders are compared. The contour lines indicate the sintering time in hours, assuming isothermal conditions. Such maps are useful as quick reference guides for designing optimal sintering cycles.

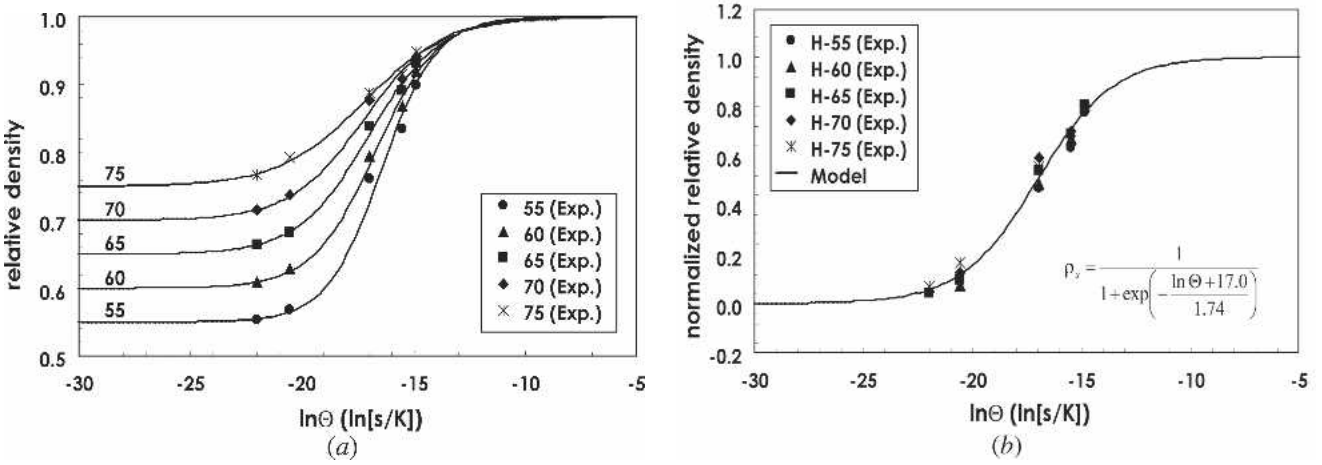


Fig. 5—Green density effects on the master sintering curve for the H-2 molybdenum powder: (*a*) raw master sintering curves for compacts fabricated to different green densities using die compaction and (*b*) normalized master sintering curve.

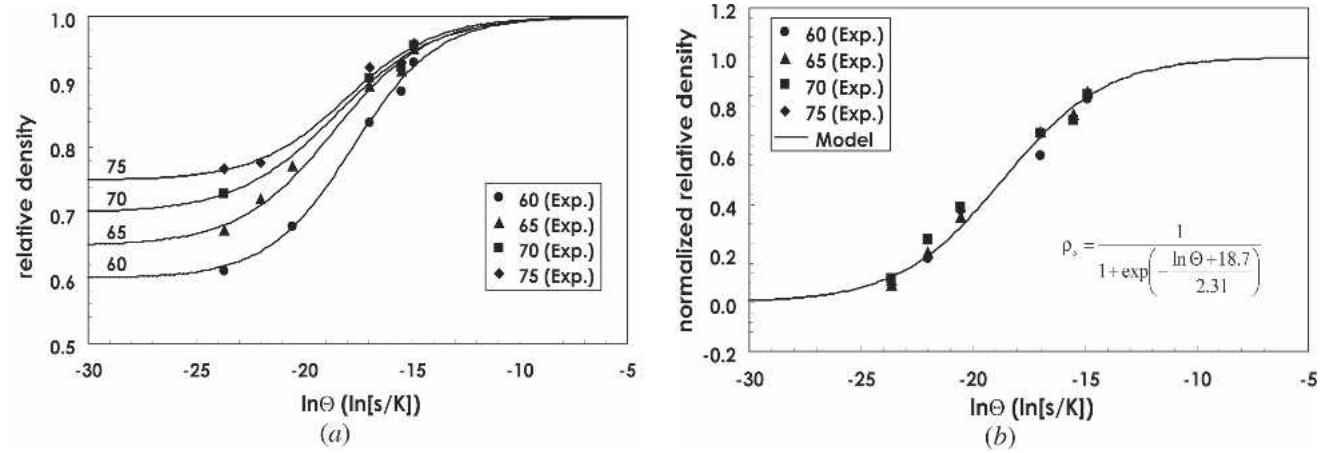


Fig. 6—Green density effects on the individual master sintering curves for the O-2 powder formed by die compaction: (*a*) raw master sintering curves for die compacted compacts of differing green densities and (*b*) normalized master sintering curve.

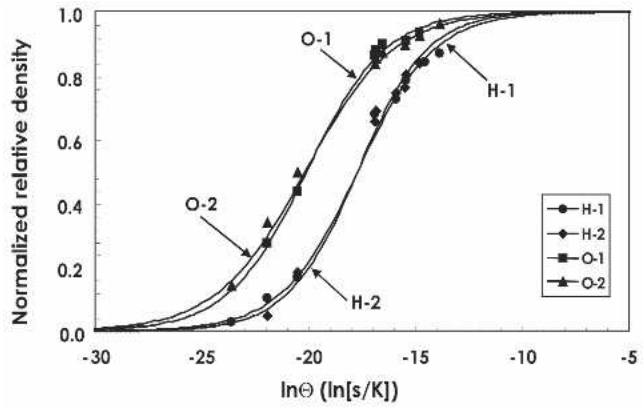


Fig. 7—Summary of all master sintering curves for molybdenum by normalizations.

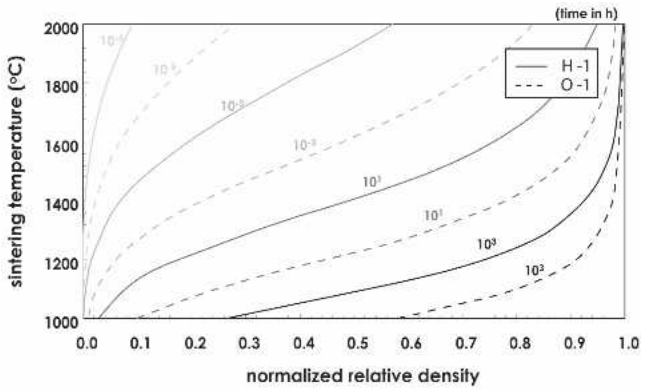


Fig. 8—Comparison of time-temperature-density plots between the H-1 and O-1 grades of injection molded molybdenum powders.

## VII. CONCLUSIONS

The sintering responses of several molybdenum powders are collapsed into normalized master sintering curves that allow inspection of how different thermal cycles impact sintered density. A new normalized master sintering curve is introduced that removes differences from the initial density, making the approach broadly applicable

to both injection molding and die compaction processes. Examples are offered on the use of these master sintering curves for assessment of different sintering conditions and demonstrations of effects linked to powder vendor, particle size, polymer burnout step, and powder agglomeration are given.

## ACKNOWLEDGMENTS

Funding for the modeling aspect of this study was provided by the National Institute for Standards and Technology through its Advanced Technology Program (Award No. 70NANB0H3019) in partnership with Polymer Technologies. The experimental portion was supported by the Picatinny Arsenal, AMSTA-AR-WEH. Finally, partial support for the program was provided by the member companies in the Penn State Center for Innovative Sintered Products. Powders were donated by Osram Sylvania and HC Starck.

## REFERENCES

1. J.D.S. Gurosik: Master's Thesis, Pennsylvania State University, University Park, PA, 2003.
2. B.H. Rabin and R.M. German: *Physical Metallurgy and Technology of Molybdenum and Its Alloys*, Symp. Proc., AMAX Materials Research Center, Ann Arbor, MI, 1986, K. Miska, M. Semchyshen, and E. Whelan, eds., pp. 101-05.
3. R.M. German and C.A. Labombard: *Int. J. Powder Metall. Powder Technol*., 1982, vol. 18 (2), pp. 147-56.
4. H. Su and D.L. Johnson: *J. Am. Ceram. Soc*., 1996, vol. 79, pp. 3211-17.
5. D.L. Johnson: *Sintering 2003*, proceedings at www.mri.psu.edu/conferences/sint03/#p1, Day 1 Plenary Session–Gary Messing.
6. R.M. German: *Sintering Theory and Practice*, John Wiley and Sons, New York, NY, 1996, p. 80.
7. R.M. German and Z.A. Munir: *J. Less-Common Met*., 1978, vol. 58, pp. 61-74.
8. R.M. German: in *Sintering—Theory and Practice*, D. Kolar, S. Pejovnik, and M.M. Ristic, eds., Elsevier Scientific, Amsterdam, The Netherlands, 1982, pp. 177-83.
9. R.M. German: *Powder Metall*., 1979, vol. 22, pp. 29-30.
10. P.E. Zovas and R.M. German: *Metall. Trans. A*, 1984, vol. 15A, pp. 1103-10.